nature genetics

SUPPLEMENTARY INFORMATION

https://doi.org/10.1038/s41588-019-0428-5

In the format provided by the authors and unedited.

Phosphorylation of histone H3.3 at serine 31 promotes p300 activity and enhancer acetylation

Sara Martire, Aishwarya A. Gogate, Amanda Whitmill, Amanuel Tafessu, Jennifer Nguyen, Yu-Ching Teng, Melodi Tastemel and Laura A. Banaszynski*

Cecil H. and Ida Green Center for Reproductive Biology Sciences and the Division of Basic Research, Department of Obstetrics and Gynecology, Children's Medical Center Research Institute, Hamon Center for Regenerative Medicine, University of Texas Southwestern Medical Center, Dallas, TX, USA.
*e-mail: laura.banaszynski@utsouthwestern.edu

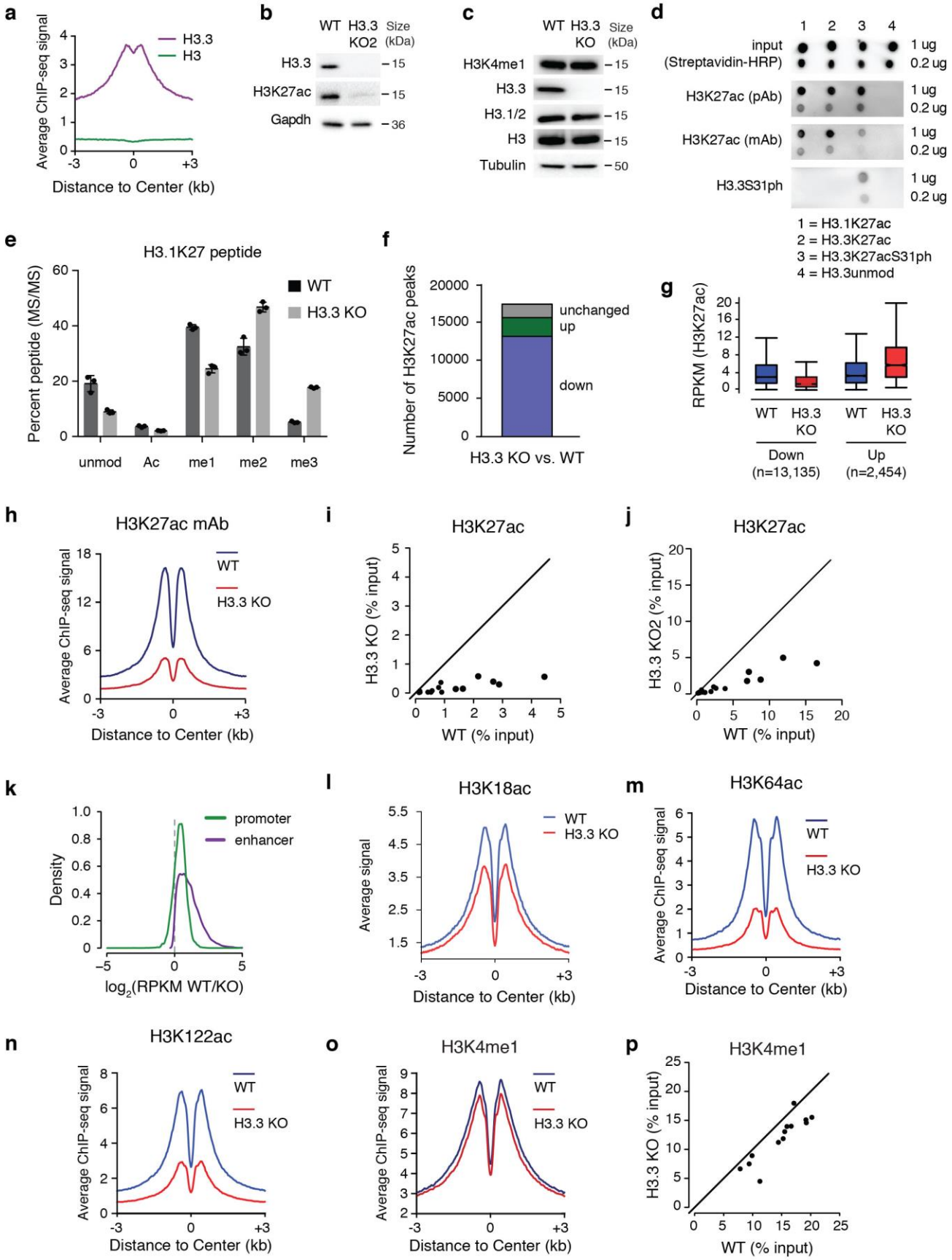
a
Average ChIP-seq signal
H3.3
H3
Distance to Center (kb)
b
WT
H3.3 KO2
Size (kDa)
H3.3
H3K27ac
Gapdh
c
WT
H3.3 KO
Size (kDa)
H3K4me1
H3.3
H3.1/2
H3
Tubulin
d
1
2
3
4
input (Streptavidin-HRP)
1 ug
0.2 ug
H3K27ac (pAb)
H3K27ac (mAb)
H3.3S31ph
1 = H3.1K27ac
2 = H3.3K27ac
3 = H3.3K27acS31ph
4 = H3.3unmod
e
H3.1K27 peptide
Percent peptide (MS/MS)
WT
H3.3 KO
unmod
Ac
me1
me2
me3
f
Number of H3K27ac peaks
unchanged
up
down
H3.3 KO vs. WT
g
RPKM (H3K27ac)
WT
H3.3 KO
WT
H3.3 KO
Down (n=13,135)
Up (n=2,454)
h
H3K27ac mAb
Average ChIP-seq signal
WT
H3.3 KO
Distance to Center (kb)
i
H3K27ac
H3.3 KO (% input)
WT (% input)
j
H3K27ac
H3.3 KO2 (% input)
WT (% input)
k
Density
promoter
enhancer
log2(RPKM WT/KO)
l
H3K18ac
Average signal
WT
H3.3 KO
Distance to Center (kb)
m
H3K64ac
Average ChIP-seq signal
WT
H3.3 KO
Distance to Center (kb)
n
H3K122ac
Average ChIP-seq signal
WT
H3.3 KO
Distance to Center (kb)
o
H3K4me1
Average ChIP-seq signal
WT
H3.3 KO
Distance to Center (kb)
p
H3K4me1
H3.3 KO (% input)
WT (% input)

Supplementary Figure 1

Histone H3.3 facilitates histone acetylation at enhancers and promoters. Related to Figure 1.

a, Average profile showing enrichment of H3 and H3.3 at promoter-distal enhancers (± 3 kb from TSS) in mESC, related to Figure 1a.
b, Immunoblot of whole cell lysates from WT and H3.3 KO2 (independent clone) mESCs. Blot is representative of three independent experiments. See also Supplementary Figure 10 for all the blots in this figure.
c, Immunoblot with the indicated antibodies of whole cell lysates from WT and H3.3 KO mESCs.
Blot is representative of three independent experiments.
d, Dot blot array showing H3K27ac antibodies reactivity for either H3.1K27ac or H3.3K27ac peptides. Blot is representative of two independent experiments.
e, Quantification of histone acetylation and methylation levels in WT and H3.3 KO mESCs by mass spectrometry (Mod SpecTM, Active Motif). Relative abundance across samples is reported. Data represented as mean ± s.d (n=3).
f, Bar graph showing the number of H3K27ac peaks that show changes in H3K27ac levels between WT and H3.3 KO mESC at enhancers (± 3 kb from TSS).
g, Boxplots showing H3K27ac enrichment levels for distal enhancers that show reduced (n=13,135) and increased (n=2,454) H3K27ac enrichment in H3.3 KO mESCs compared to WT. The bottom and top of the boxes correspond to the 25th and 75th percentiles, and the internal band is the 50th percentile (median). The plot whiskers correspond to 1.5× interquartile range and outliers are excluded.
h, Average profile of H3K27ac enrichment at enhancers in WT and H3.3 KO mESCs using a monoclonal antibody.
i,j, ChIP-qPCR validation from independent experiments of H3K27ac enrichment at 16
enhancers in WT and 2 clonal H3.3 KO mESCs.
k, Ratio (log2) of H3K27ac enrichment in WT versus H3.3 KO mESCs at promoters and
enhancers showing reduced acetylation in the absence of H3.3. x axis values > 0 indicate reduced H3K27ac enrichment in the absence of H3.3.
l,m,n, Average profile of H3K18ac (l) H3K64ac (m) and H3K122ac (n) enrichment at enhancers in WT and H3.3 KO mESCs.
o,p, Average profile (o) and ChIP-qPCR validation (p) of H3K4me1 enrichment at enhancers in WT and H3.3 KO mESCs.

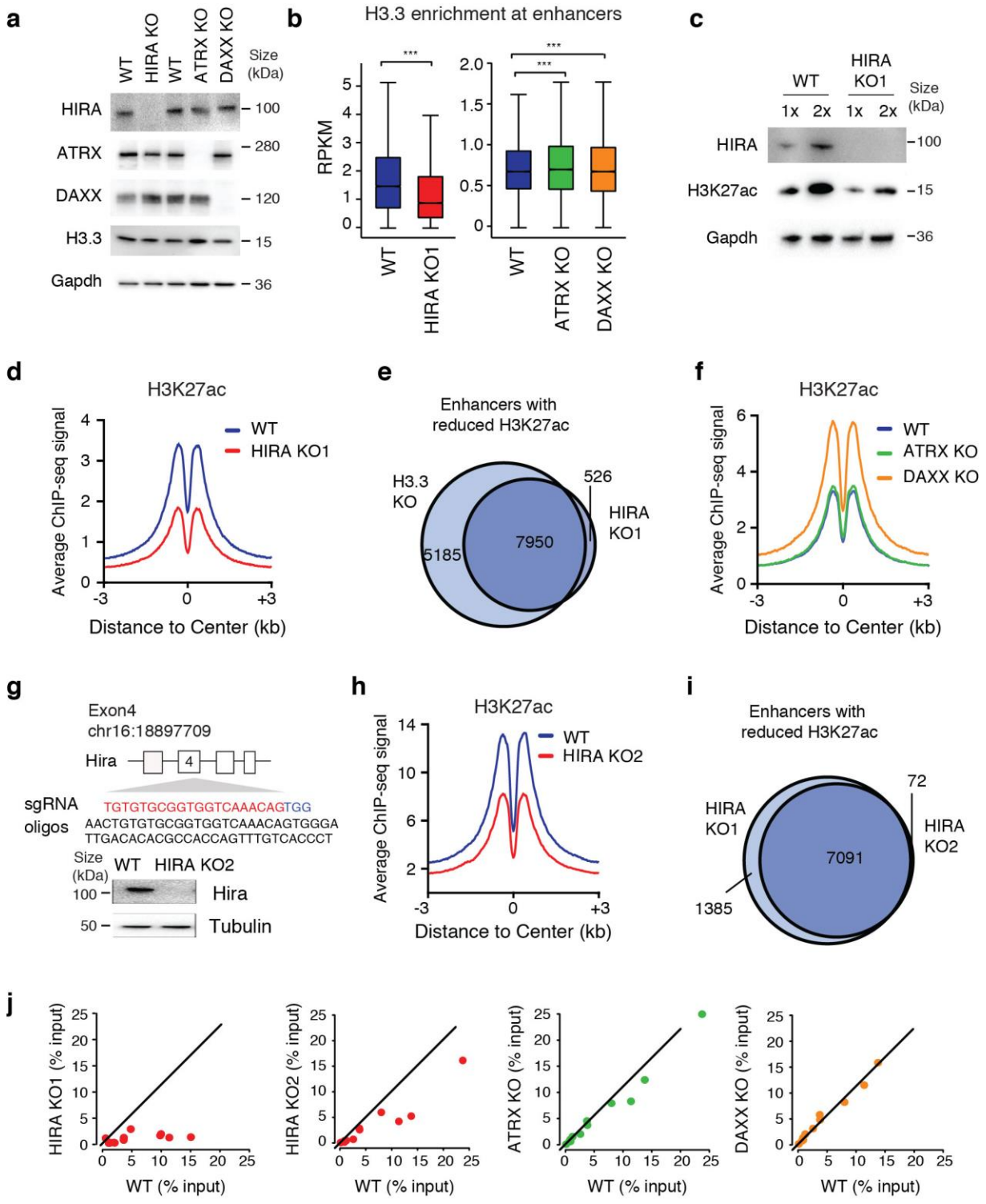

Supplementary Figure 2

H3K27ac at enhancers is facilitated by HIRA-dependent H3.3 deposition. Related to Figure 1.

a, Immunoblot with the indicated antibodies of whole cell lysates from WT and HIRA, ATRX and DAXX KO mESCs. Blot is representative of three independent experiments. See also Supplementary Figure 11 for all the blots in this figure.

b, Boxplot showing H3.3 enrichment at enhancers in WT and HIRA, ATRX and DAXX KO mESCs (n = 17,589). WT & HIRA KO $P < 2.2$

$\times 10^{-16}$, WT & ATRX KO $P = 1.664 \times 10^{-14}$, WT & DAXX KO $P = 0.0007246$ by Wilcoxon rank sum two-side test. The bottom and top of the boxes correspond to the 25th and 75th percentiles, and the internal band is the 50th percentile (median). The plot whiskers correspond to 1.5× interquartile range and outliers are excluded.

c, Immunoblot with the indicated antibodies from WT and HIRA KO mESCs whole cell lysates loaded with increased protein concentration (1x, 2x). Blot is representative blot of two independent experiments.

d, Average profile of H3K27ac enrichment at enhancers in WT and HIRA KO mESCs.

e, Venn diagram showing overlap between H3.3 KO and HIRA KO reduced H3K27ac peaks.

f, Average profile of H3K27ac enrichment at enhancers in WT, ATRX KO, and DAXX KO mESCs.

g, Schematic of CRISPR/Cas9 strategy for generation of HIRA KO mESCs and immunoblot showing complete loss of HIRA. Blot is representative of four independent experiments.

h, Average profile of H3K27ac enrichment in WT and HIRA KO2 mESCs at distal enhancers.

i, Venn diagram showing overlap between HIRA KO and HIRA KO2 reduced H3K27ac peaks.

j, ChIP-qPCR validation from independent experiments of H3K27ac enrichment at enhancers in all four chaperone KO mESCs line compared to the corresponding WT mESCs.

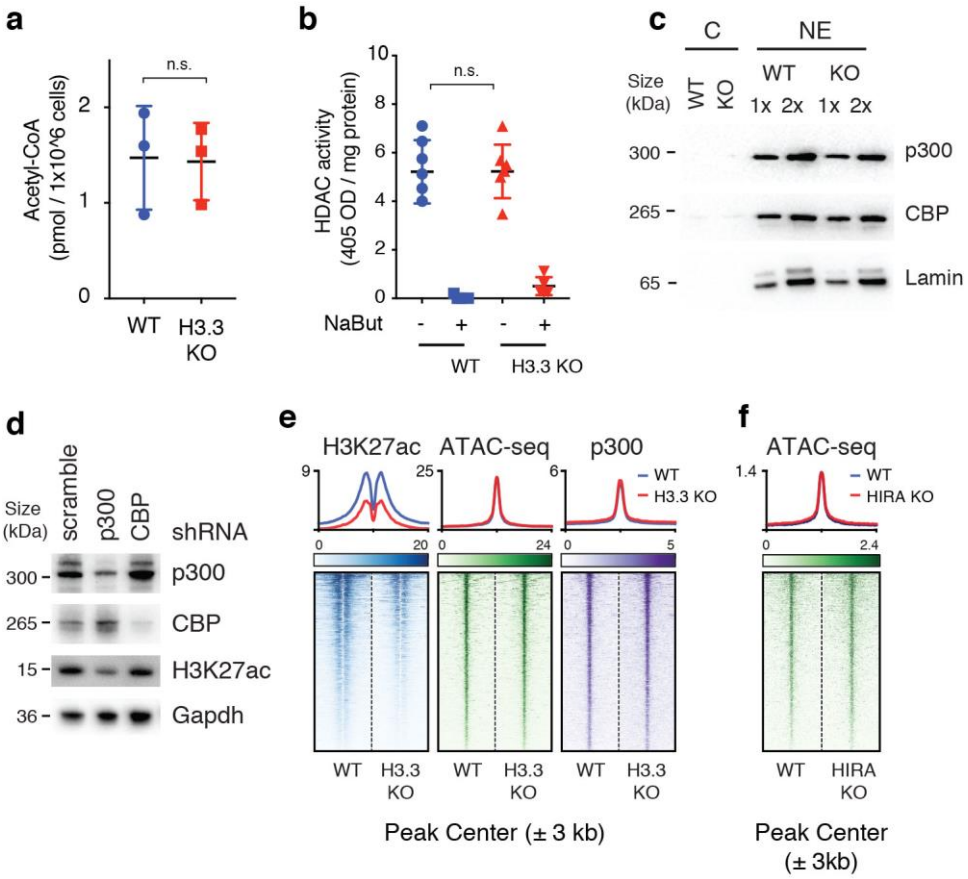

Supplementary Figure 3

H3.3 loss does not alter chromatin accessibility or p300 recruitment. Related to Figure 2.

a, Quantification of Acetyl-CoA levels from 5×10^6 cells (Sigma MAK039) in WT and H3.3 KO mESC. Data represented as mean ± s.d. (n=3), two-tailed t-test, n.s. = 0.9.

b, HDAC activity (BioVision K331-100) in WT and H3.3 KO mESC nuclear extracts in the presence or absence of the HDAC inhibitor Sodium Butyrate (NaBut). Data represented as mean ± s.d. (n=5), two-tailed t-test, , n.s. = 0.45.

c, Immunoblot of cytoplasmic (C) and nuclear extracts (NE) from WT and H3.3 KO mESCs. Blot is representative of three independent experiments. See also Supplementary Figure 11b.

d, Immunoblot of whole cell lysates from WT mESCs transfected with p300 and CBP shRNA. Blot is representative of four independent experiments. See also Supplementary Figure 11b.

e, Heatmaps and average profiles of H3K27ac (left), ATAC-seq (middle), and p300 (right) enrichment in WT and H3.3 KO mESCs at enhancers. 3kb around the center of enhancers are displayed for each analysis. Each row represents a single enhancer (n =17,589).

f, Heatmap and average profile of ATAC-seq in WT and HIRA KO mESCs at enhancers. 3kb around the center of enhancers are displayed for each analysis. Each row represents a single enhancer (n = 17,589).

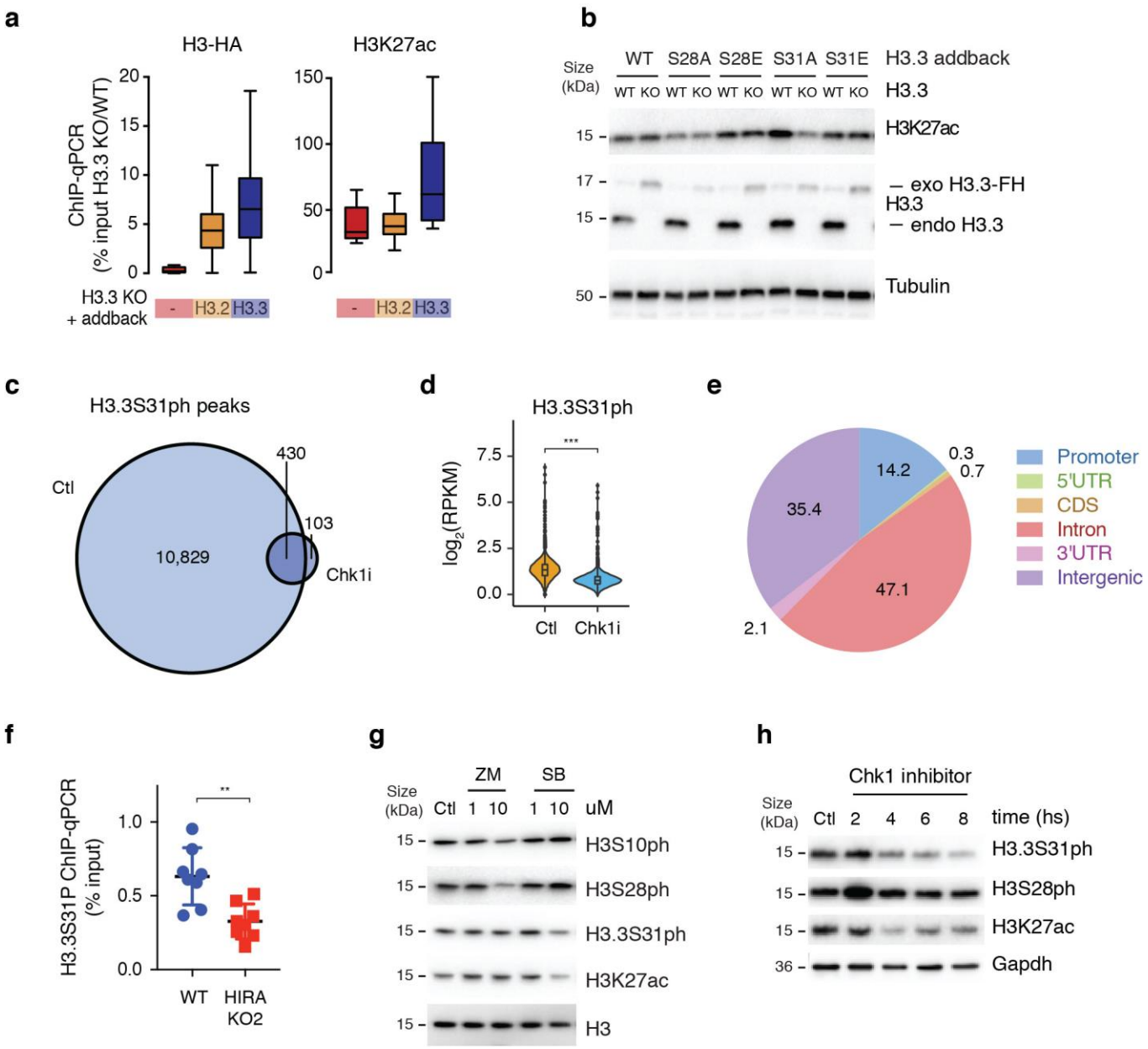

Supplementary Figure 4

H3.3 phosphorylation promotes acetylation at enhancers. Related to Figure 2.

a, Boxplots showing H3-Flag-HA (left) and H3K27ac (right) enrichment (ChIP-qPCR) at 10 enhancer regions in H3.3 KO mESCs expressing exogenous histones (H3.2 and H3.3) compared to WT mESCs. (n = 10). The bottom and top of the boxes correspond to the 25th and 75th percentiles, and the internal band is the 50th percentile (median). The plot whiskers correspond to 1.5× interquartile range and outliers are excluded.

b, Immunoblot of whole cell lysates from WT and H3.3 KO mESCs exogenously expressing histones and indicated histone mutants. Blot is representative of two independent experiments. See also Supplementary Figure 12a for all the blots in this figure.

c, Venn diagrams showing drastically reduced H3.3S31ph peaks in WT mESC treated with Chek1inhibitor (Chk1i). p = 6.419 x 10-^{14} by hypergeometric test. Ctrl peaks (n=11,259), Cheki peaks (n=533).

d, Violin plot showing H3.3S31ph in WT and mESC treated with Chek1 inhibitor (Chk1i). ***$P < 2.2 \times 10^{-16}$ by Wilcoxon rank sum two-side test (n=11,259). Violin plots displayed as boxplot in panel a.

e, Genome-wide distribution of H3.3S31ph binding sites (percent of total number of sites. H3.3S31ph ChIP-seq identified elements that

fell within 300 kb from coding regions were analyzed based on their distance from nearest genes using CEAS. The pie chart represents percent distribution.

f, ChIP-qPCR of H3.3S31ph enrichment at enhancers in WT and HIRA2 KO mESCs. Data are expressed as percentage of input and represent mean ± s.d. (n = 8), two-tailed t-test $^{**}P = 0.0016$.

g, Immunoblot of whole cell lysates from WT mESCs treated with indicated concentration of Chk1 kinase inhibitor (SB218078, “SB”) or Aurora B kinase inhibitor (ZM447439, “ZM”) for 4 hrs. Blot is representative of three independent experiments.

h, Immunoblot of whole cell lysates from wild-type mESCs treated with Chk1 inhibitor for the indicated times. Blot is representative of three independent experiments.

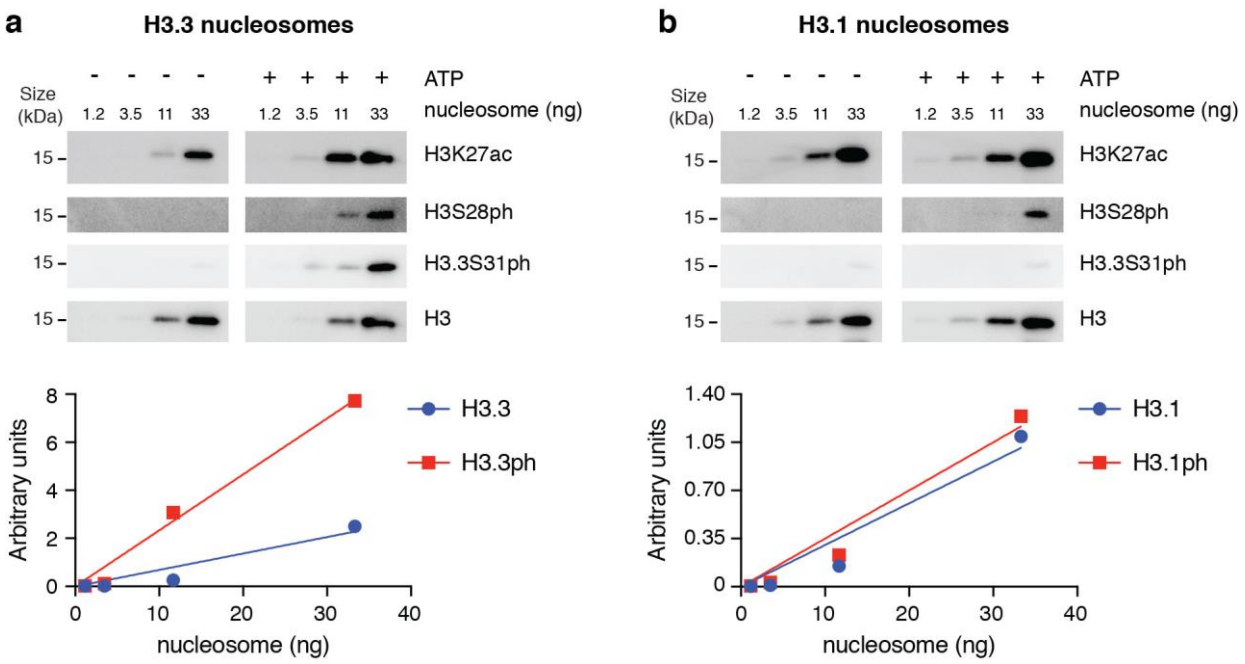

Supplementary Figure 5

H3.3-specific phosphorylation stimulates p300 histone acetyltransferase activity. Related to Figure 3.

a-b, Immunoblot (above) and densitometry (below) of p300 histone acetyltransferase assay using increasing concentrations of recombinant H3.3 (a) or H3.1 (b) nucleosomes that were preincubated with Chk1 with or without ATP. Blot is representative of three independent experiments. See also Supplementary Figure 12b.

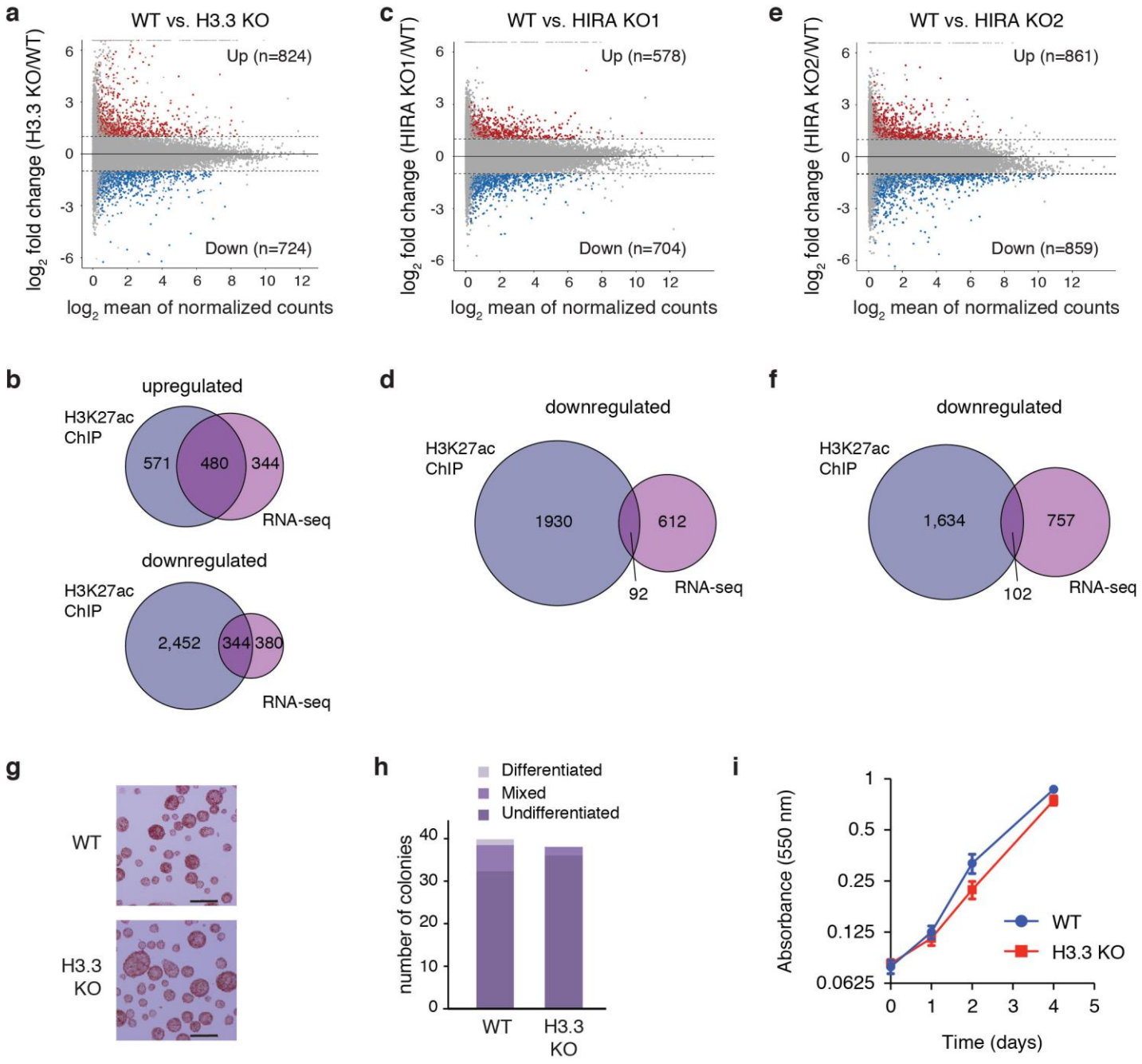

Supplementary Figure 6

mESCs depleted of H3.3 maintain self-renewal properties. Related to Figure 4.

a,c,e, MA plot of gene expression in WT and H3.3 KO (a), HIRA KO1 (c), HIRA KO2 (e) mESCs. The x-axis indicates gene counts and the y-axis represents the log2 fold change in expression for KO versus WT mESCs. Genes in red and blue were differentially expressed ($P < 0.05$) with a fold change > 2.

b, Venn diagrams showing the relationship between H3K27ac ChIP-seq and RNA-seq for regions that showed upregulation (top) or downregulation (bottom) in the absence of H3.3 in both data sets. Up regulated genes $P = 6.419 \times 10^{-14}$ and down regulated genes $P = 3.581 \times 10^{-12}$ by hypergeometric test. H3K27ac Up-regulated (n=1,051), RNA-Seq Up-regulated (n=824), H3K27ac Down-regulated (n=2,796), RNA-Seq Down-regulated (n=724).

d,f, Venn diagrams showing the relationship between H3K27ac ChIP-seq and RNA-seq for regions that showed downregulation in the

absence of H3.3 in HIRA KO cells. Down regulated genes P = 3.581 × 10-12 by hypergeometric test. (d) H3K27ac Down-regulated (n=2,022), RNA-Seq Down-regulated (n=704). (f) H3K27ac Down-regulated (n=1736), RNA-Seq Down-regulated (n=859).

g, Alkaline phosphatase staining of WT and H3.3 KO mESCs in 2i/SL media. Scale bar = 200 μm. Image is representative of three independent experiments.

h, Quantification of colony formation assay of WT and H3.3 KO mESCs.

i, Growth curve of WT and H3.3 KO mESCs assessed using MTT assay at indicated times. Data represent mean ± s.d (n=4).

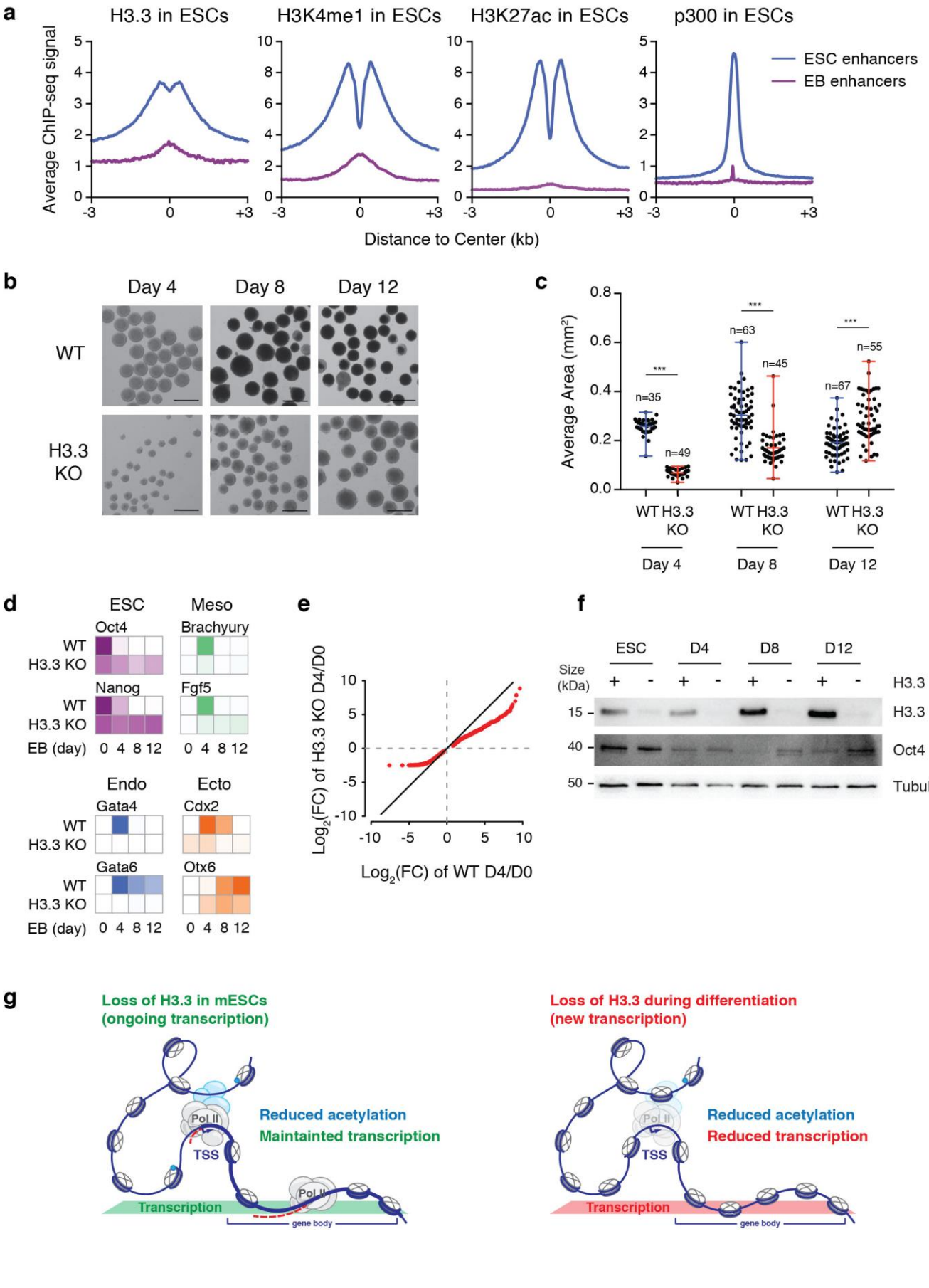
a
H3.3 in ESCs
H3K4me1 in ESCs
H3K27ac in ESCs
p300 in ESCs
Average ChIP-seq signal
ESC enhancers
EB enhancers
Distance to Center (kb)
b
Day 4
Day 8
Day 12
WT
H3.3 KO
c
Average Area (mm²)
n=35
n=49
n=63
n=45
n=67
n=55
***
WT H3.3 KO
Day 4
Day 8
Day 12
d
ESC
Meso
Oct4
Brachyury
Nanog
Fgf5
WT
H3.3 KO
EB (day) 0 4 8 12
Endo
Ecto
Gata4
Cdx2
Gata6
Otx6
e
Log2(FC) of H3.3 KO D4/D0
Log2(FC) of WT D4/D0
f
ESC
D4
D8
D12
Size (kDa)
H3.3
Oct4
Tubulin
g
Loss of H3.3 in mESCs
(ongoing transcription)
Pol II
TSS
Reduced acetylation
Maintainted transcription
Transcription
gene body
Loss of H3.3 during differentiation
(new transcription)
Reduced acetylation
Reduced transcription

Supplementary Figure 7

H3.3 Is required for mESC differentiation. Related to Figure 4.

a, Average profiles of H3.3, H3K4me1, H3K27ac and p300 enrichment in WT mESC at mESC and EBs enhancers. 3kb around the center of enhancers are displayed for each analysis.
b, Brightfield images of embryoid body (EB) differentiation in WT and H3.3 KO cells at 4, 8 and 12 days. Scale bar = 1 mm. Image is representative of at least three independent experiments.
c, Comparison of average areas of WT and H3.3 KO embryoid bodies at the indicated days of differentiation. Data represent the mean ± s.d., two-tailed t-test ***$P = 7.52^{-53}$, **$P = 0.0068$, ***$P = 0.00016$.
d, Heatmap representation of transcript levels (RT-qPCR) of markers of pluripotency (ESC) (Oct4, Nanog), mesoderm (Brachyury, Fgf5), endoderm (Gata4, Gata6) and ectoderm (Cdx2, Otx6) during EBs differentiation. e, Comparison of transcription changes at day 4 of EB differentiation for WT and H3.3 KO cells. Gene list represent genes whose expression decreases or increases in expression upon differentiation compared to WT ESCs. The x- and y-axis represent the fold change (log2) of RNA expression between D4 and D0 in WT and H3.3 KO, respectively.
f, Immunoblot of H3.3 and Oct4 in WT and H3.3 KO embryoid bodies at the indicated days of differentiation. Blot is representative of two independent experiments. See also Supplementary Figure 12c.
g, Model figure representing differential requirement for H3.3 during ongoing transcription (left) and the initiation of transcription (right).

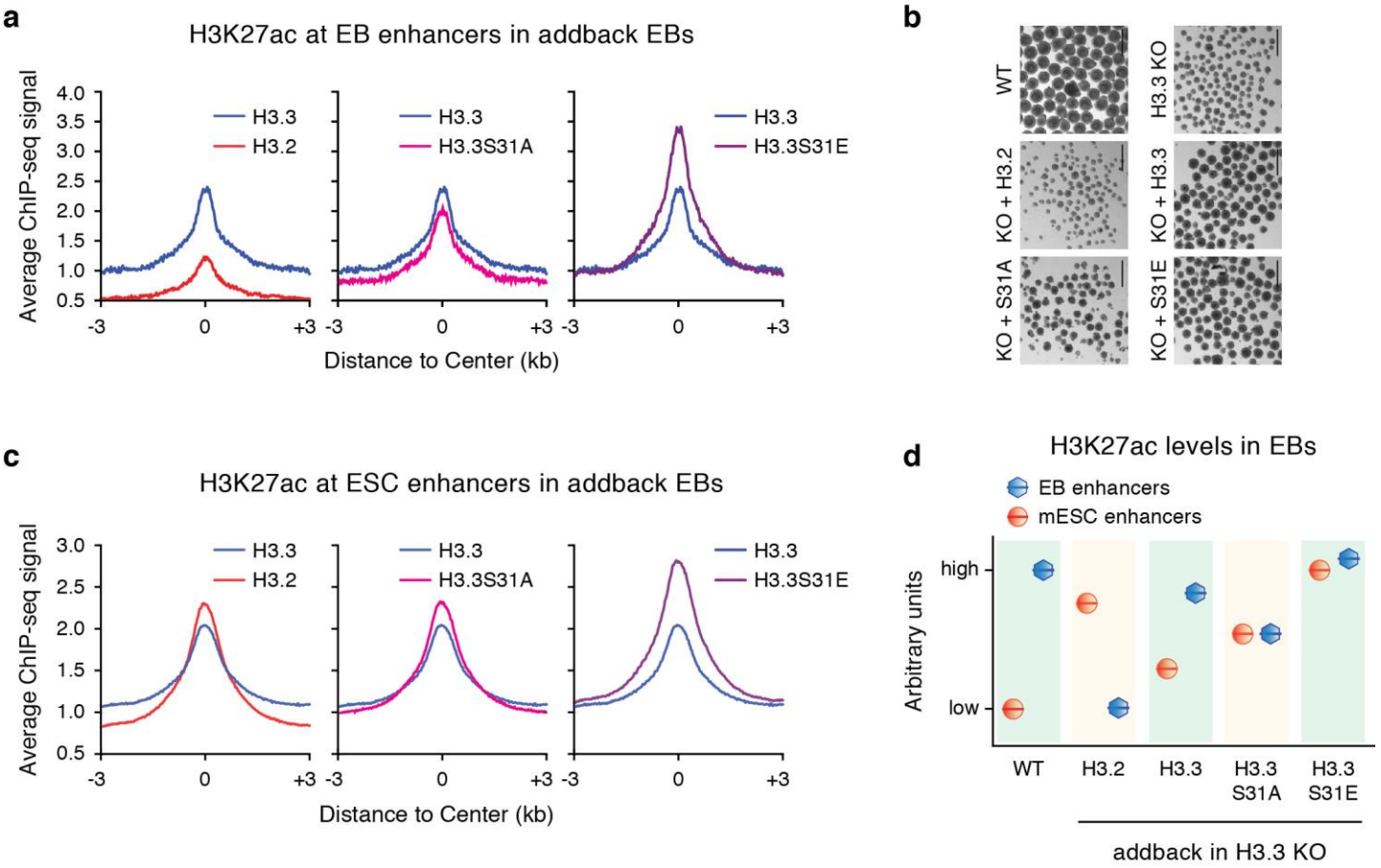

Supplementary Figure 8

H3.3 phosphorylation promotes enhancer acetylation during differentiation. Related to Figure 4.

a, Average profiles of H3K27ac enrichment at EB enhancers in H3.3KO EBs expressing the indicated exogenous protein. 3kb around the center of enhancers are displayed for each analysis.

b, Brightfield images of EB differentiation in WT and H3.3 KO cells and in H3.3 KO cells expressing exogenous histone mutants at day 4. Scale bar = 1 mm. Image is representative of three independent experiments.

c, Average profiles of H3K27ac enrichment at ESC enhancers in H3.3KO EBs expressing the indicated exogenous protein. 3kb around the center of enhancers are displayed for each analysis.

d, Schematic of H3K27ac levels in WT and in H3.3 KO cells expressing exogenous histone mutants at day 4 of differentiation at mESC (pluripotency-specific) and EB (differentiation-specific) enhancers.

a

Fig. 1b

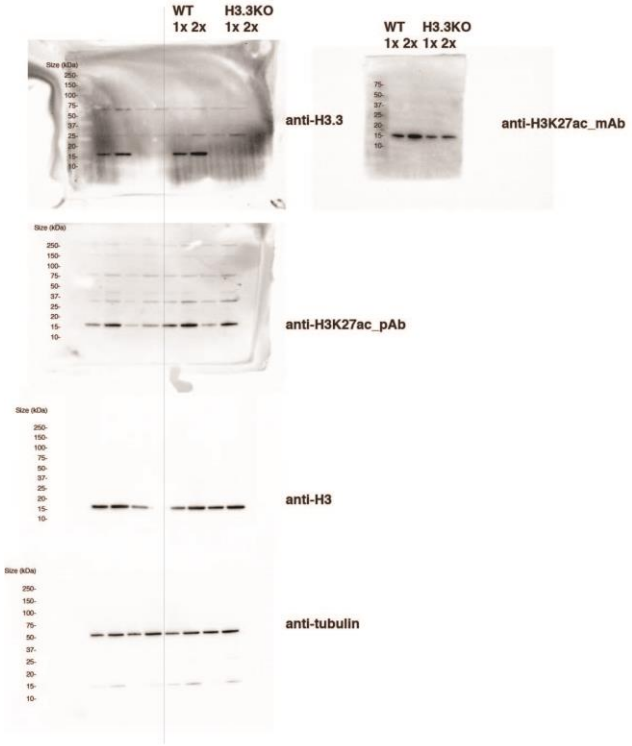

b

Fig. 2a

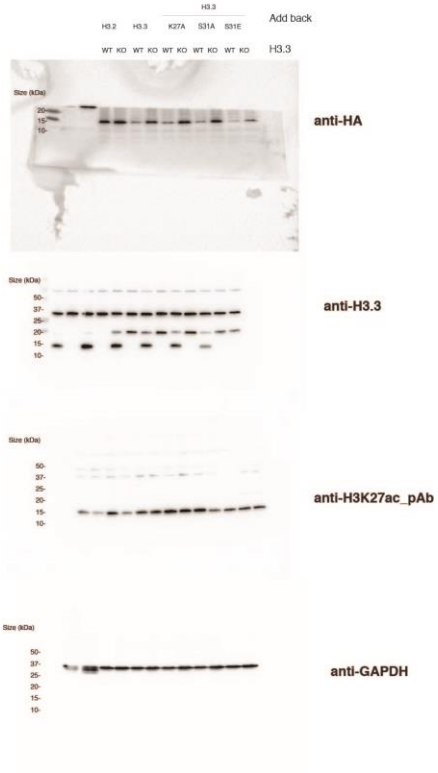

c

Fig. 3a

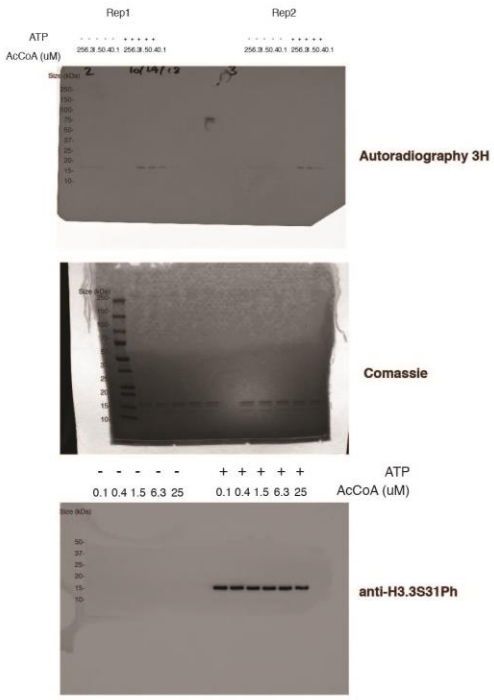

Fig. 3b

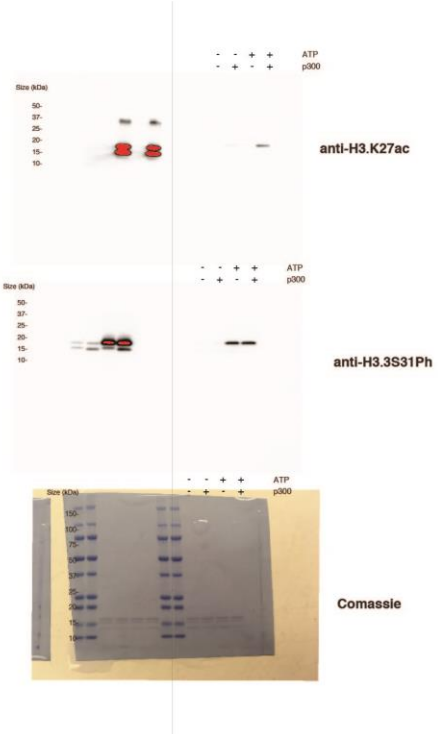

Supplementary Figure 9

Raw immunoblots related to main figures.

a, Western blots related to Figure 1b
b, Western blots related to Figure 2a
c, Western blots related to Figure 3a,b

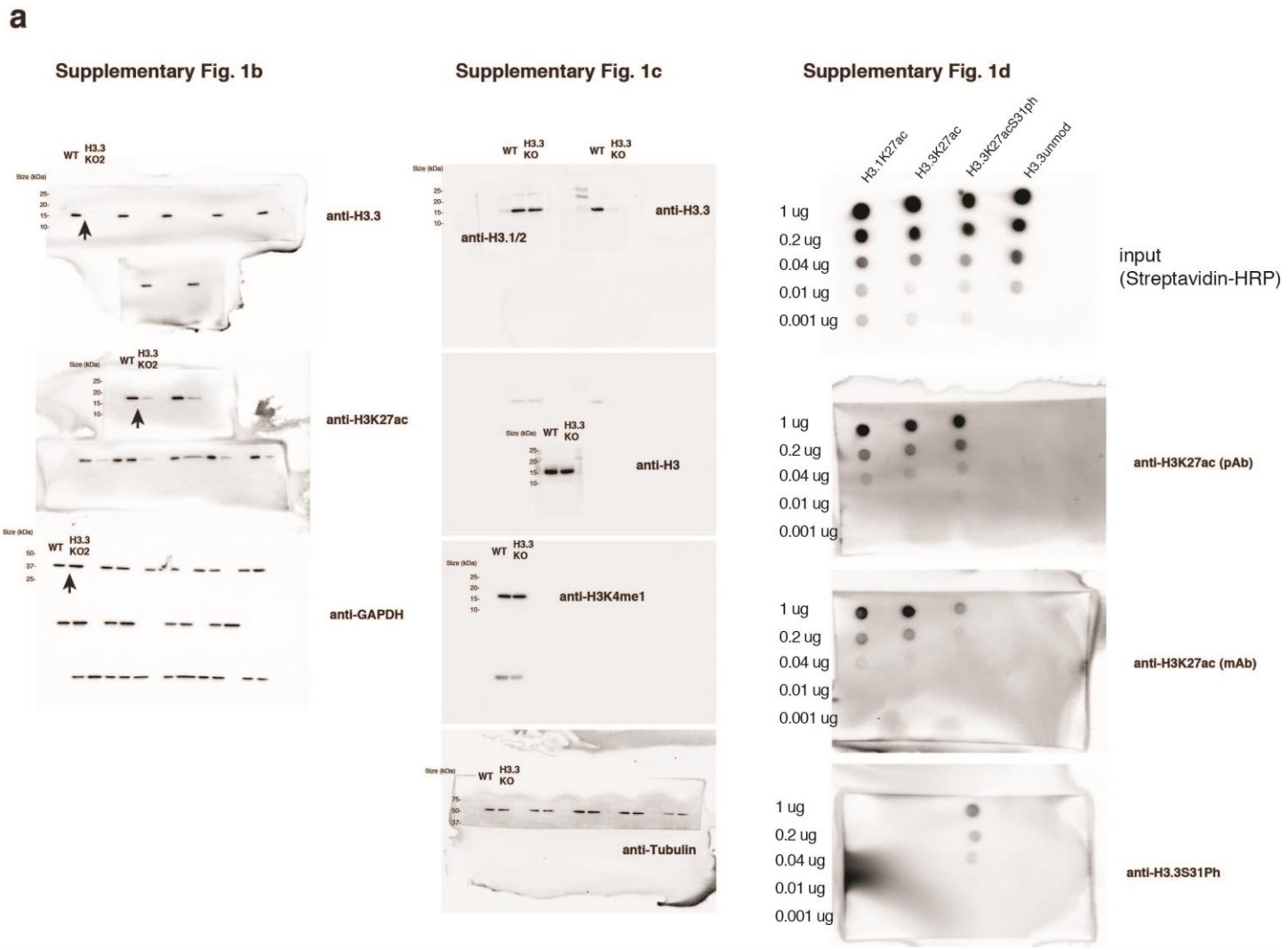

Supplementary Figure 10

Raw immunoblots.

a, Western blots related to Supplementary Figure 1b,c,d

a

Supplemetary Fig. 2a

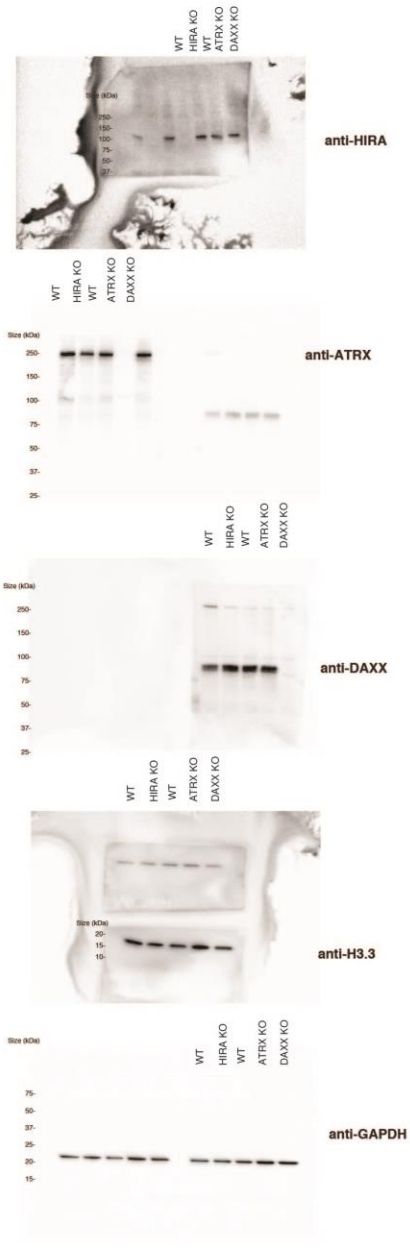

Supplementary Fig. 2c

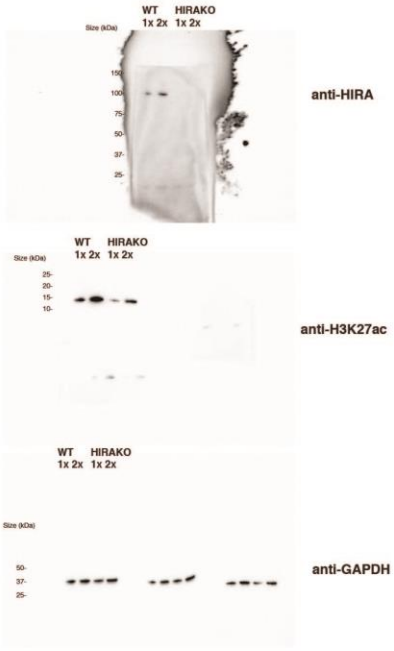

Supplemetnary Fig. 2g

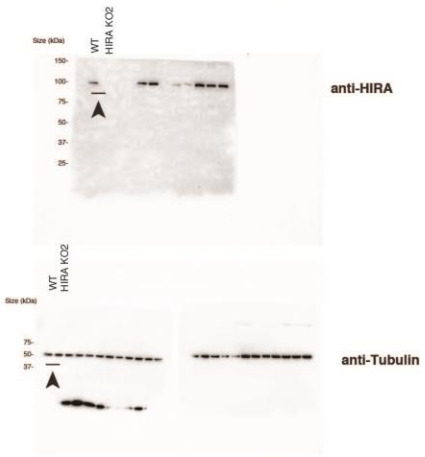

b

Supplementary Fig. 3c

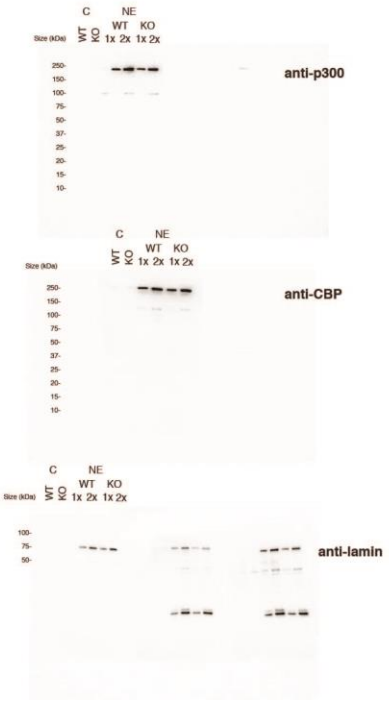

Supplementary Fig. 3d

Supplementary Figure 11

Raw immunoblots.

a, Western blots related to Supplementary Figure 2a,c,g
b, Western blots related to Supplementary Figure 3c,d

a

Supplementary Fig. 4b

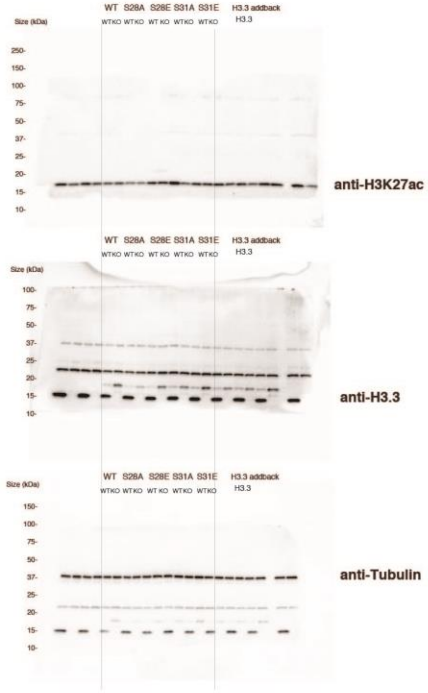

Supplementary Fig. 4g

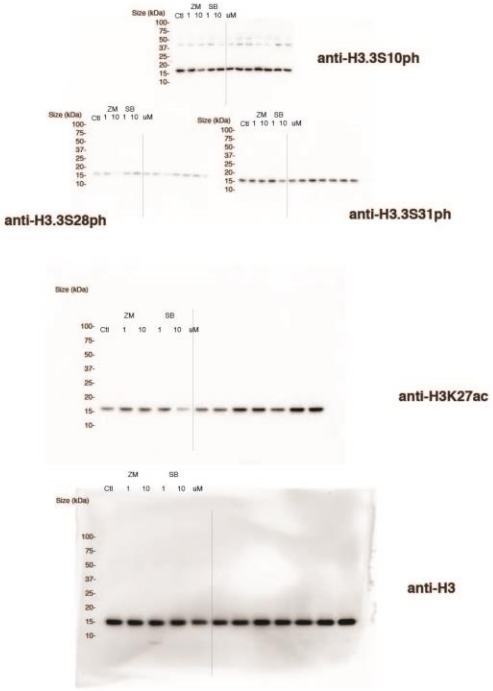

Supplementary Fig. 4h

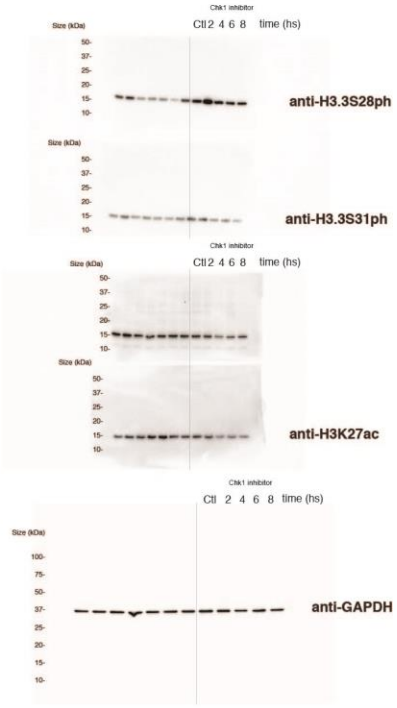

b

Supplementary Fig. 5a/b

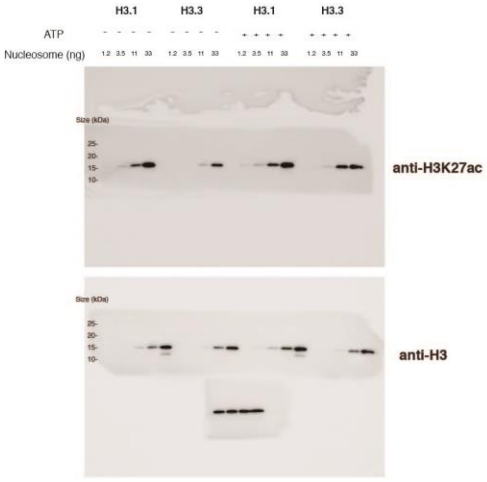

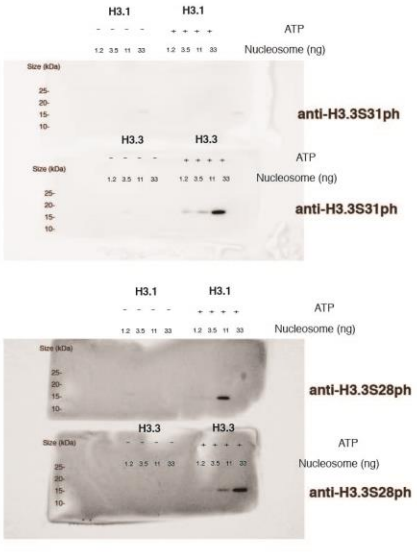

c

Supplementary Fig. 7f

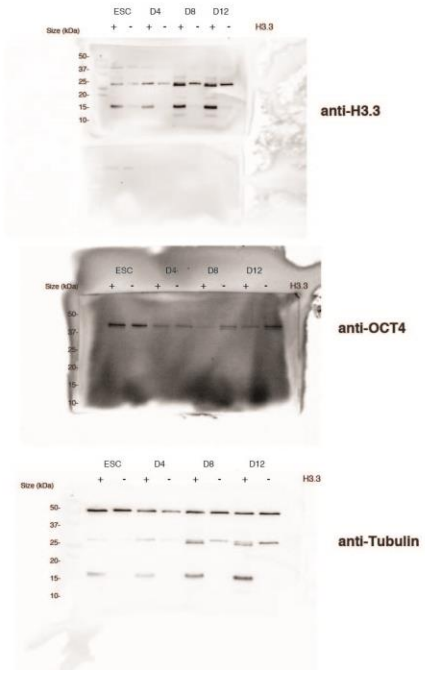

Supplementary Figure 12

Raw immunoblots.

a, Western blots related to Supplementary Figure 4b,g,h
b, Western blots related to Supplementary Figure 5a,b
c, Western blots related to Supplementary Figure 7f

Although acetylation has long been correlated with gene expression, we find that reduced acetylation is well-tolerated in mESCs. It is possible that under normal conditions enhancers are acetylated more robustly than is required for a functional readout of this modification. Such "buffering" could explain why a global ~2-fold loss in H3K27ac levels has modest effect on transcription. Our data are also inclusive of a model in which enhancer acetylation plays different roles in the activation *vs*. maintenance of transcription, analogous in some ways to different chromatin-based mechanisms that support the initiation and maintenance of X inactivation[1]. We cannot exclude that lack of H3.3 may affect the rate of transcription, pausing or other transcription-related events, which deserves greater study[2]. Regardless, we observe that cells lacking H3.3 show reduced capacity in establishing acetylation at enhancers that are activated upon differentiation, with corresponding reduced expression from nearby genes.

1. Galupa, R. & Heard, E. X-Chromosome Inactivation: A Crossroads Between Chromosome Architecture and Gene Regulation. *Annu. Rev. Genet.* **52,** 535–566 (2018).
2. Zhang, H. *et al.* RPA Interacts with HIRA and Regulates H3.3 Deposition at Gene Regulatory Elements in Mammalian Cells. *Mol. Cell* **65,** 272–284 (2017).